J Appl Biotechnol Rep. 2020 Mar;7(1):32-40

doi 10.30491/JABR.2020.105918

Journal of
Applied Biotechnology
Reports

Original Article

Characterization and Investigation of Antibacterial Activity of Injectable Hydroxyapatite-Alginate Hydrogel

Masoud Babaei Forootan[1], Abbas Ali Imani Fooladi[2], Hamid Tebyanian[3], Mahdi Fasihi-Ramandi[4], Sepehr Dehghan[1], Mohammad Reza Nourani[1*]

[1]Nanobiotechnology Research Center, Baqiyatallah University of Medical Sciences, Tehran, Iran
[2]Applied Microbiology Research Center, Systems Biology and Poisonings Institute, Baqiyatallah University of Medical Sciences, Tehran, Iran
[3]Research Center for Prevention of Oral and Dental Diseases, Baqiyatallah University of Medical Sciences, Tehran, Iran
[4]Molecular Biology Research Center, Systems Biology and Poisoning Institute, Baqiyatallah University of Medical Sciences, Tehran Iran

Corresponding Author: Mohammad Reza Nourani, PhD, Professor, Nanobiotechnology Research Center, Baqiyatallah University of Medical Sciences, Tehran, Iran. Tel: +98-9124404539, Emali: r.nourani@yahoo.com

Received May 25, 2019; **Accepted** November 11, 2019; **Online Published** March 11, 2020

Abstract

Introduction: Bone replacement materials used for void filling and healing the bone injuries with antibacterial characteristics is of interest to many researchers. The main inorganic material in human and animal bones makes calcium phosphate suitable to interact with neighboring bones and enhances the healing process. A few drawbacks of using neat Ca/P powder such as low solubility and its brittle nature makes it difficult to manipulate. Therefore, the composition of these bio-ceramics with biopolymers makes an ideal injectable mixture with proper mechanical properties. In this study a hybrid composite of sodium alginate (SA) and calcium phosphate was prepared and its antibacterial characteristics were investigated.

Materials and Methods: In this study, hydrogel composites of SA/brushite and SA/hydroxyapatite (HA) were fabricated with different fabrication methods as well as the final compositions. The filler properties of these hybrid composites were investigated using X-ray diffraction (XRD), Fourier transform infrared (FTIR) and scanning electron microscopy (SEM). Also, to determine the antibacterial effects, the minimal inhibitory concentration (MIC) and minimal bactericidal concentration (MBC) were assessed on two strands of microorganisms including *Escherichia coli* and *Streptococcus agalactiae* which are known as causative agents for biofilm formation on implant surfaces.

Results: Findings reveal that calcium phosphate in the form of brushite in combination with alginate and carboxy-methyl-cellulose (CMC) has intrinsic antibacterial efficiency in concentrations lower than 250 µg/mL.

Conclusions: The composition of SA/brushite with CMC carrier is a promising injectable filler with antibacterial properties which could be used to treat bone injuries and orthopedic applications.

Keywords: Antibacterial, Bone Filler, Hydroxyapatite, Scaffold, Alginate, Brushite

Citation: Babaei Forootan M, Imani Fooladi AA, Tebyanian H, Fasihi-Ramandi M, Dehghan S, Nourani MR. Characterization and investigation of antibacterial activity of injectable hydroxyapatite-alginate hydrogel. J Appl Biotechnol Rep. 2020;7(1):32-40. doi:10.30491/JABR.2020.105918.

Introduction

Every year, millions of people around the world suffer from bone injuries. Yet, bone replacement materials were used to fill or repair bone defects resulting from traumatic insult, tumor ablation or congenital deformities over the past few decades.[1-4] However, healing these defects with the ability to induce and conduct bone formation with less operational surgeries even for complex defect geometries is still a vital challenge for surgeons. In many cases, allograft, autologous bone grafts and xenografts are used which may lead to more complicated therapeutic procedures due to infections or immunobiology failure by host.[5] Therefore, in the past 50 years, many scientific efforts have been made to make some appropriate bone substitute materials.[6-10] Since human bones consist of 65% hydroxyapatite (HA), many researches are inclined to use and include calcium phosphates in their compositions to mimic their role in natural bone structure.[11,12] Among these material, calcium phosphates HA, beta-tricalcium phosphate and their composite named biphasic calcium phosphate are of interest due to their biocompatibility, osteoconductivity and osteoinductivity properties.[13] Considering its close similarity to inorganic material in human and animal bones, HA would be a suitable option to interact with neighboring bones and it would also enhance the healing process.[14] Moreover, HA has been found to be an effective substrate for cell attachment and expression of osteoblast phenotypes.[15,16] However, it remains in the body for a long time due to its low biodegradability. Therefore, there are a few drawbacks in using neat HA powder such as low solubility which prolongs the degradability process or its brittle nature which makes it difficult for surgeons to use

Copyright © 2020 The Author(s). This is an open-access article distributed under the terms of the Creative Commons Attribution License (http://creativecommons.org/licenses/by/4.0), which permits unrestricted use, distribution, and reproduction in any medium, provided the original work is properly cited.

and manipulate and even it could cause a secondary fracture.[17] Subsequently, biopolymers which are also biocompatible, abundant in source and possess various chemical, physical or mechanical properties could be good options as polymer matrix hosts for inorganic powders such as HA. Moreover, strong interfacial interaction between the inorganic phase and biopolymer matrix via electrostatic interactions and hydrogen bonding will create a synergistic effect which enhances the mechanical stability and manipulation. These compositions are potent enough to be loaded by drugs or used as a paste for bone substitution.[6,7] On the other hand, alginate is a biocompatible and degradable polysaccharide which is derived from brown sea algae and is well known for its good ability to form a scaffold via ionic interaction. Also, the existing carboxy groups in polysaccharide chains would interact with their opposite charged ions and would form a 3D gel network.[18] Therefore, this capability could be used to form an in-situ hydrogel which is especially suitable for a large bone defect filling when it comes to be mixed with a biogenic material such as HA.[19-21] Accordingly, there are few reports in recent years which describe the preparation and characterization of sodium alginate (SA) consisting of calcium phosphate composites with a focus on HA as a constituent of their mineral component.[7,19-23] Thus, different properties of these composites are well documented in these studies. In the same vein, Luo et al have investigated the effect of surface treatment of nano-plate shaped HA reinforced by SA scaffolds containing glucosamine which was designed for bone tissue engineering applications.[23] In this study, glucosamine was grafted on the surface of HA via intercalation method. Eventually, it was found out that the incorporation of glucosamine grafted HA in the SA matrix improves its compressive strength as well as the promotion of MG-63 cell's proliferation.[23] The mechanical strength is of importance to fabricate gels with good manipulating properties. On the other hand, Benedini et al have looked into pH adaptation capability of HA/SA to ensure its stability during its contact with body fluid.[22] They were able to demonstrate that the decrease in pH value of media (such as the one which happens in a bone defect) will not lead to the degradation of composite unlike the behavior previously observed in traditional gels. Also, by adjusting the proper incubation time in a simulated body fluid and the amount of introduced synthetic HA, it is possible to improve the development of biogenic HA. Recently, brushite has been proposed as a new hybrid material in combination with alginate. It is worth mentioning that brushite (dicalcium phosphate dehydrate) is a member of calcium phosphates with Ca/P ratio of one. Moreover, brushite is biodegradable and can be resorbed in a physiological condition which would make it a suitable choice to be used in many areas such as bone cements, fillers and drug delivery systems.[24-26] In addition, CaP cements are usually composed of HA or brushite.[24,27] Consequently, the higher solubility of brushite leads to more resorbable cements and therefore, brushites have received considerable attention.[28,29] Also, brushite naturally could be found in pathological calcifications.[30] Alternatively, the other form of dicalcium phosphates is montite with the same Ca/P ratio of brushite but only in dried conditions which can be precipitated by the dehydration of brushite. Despite the fact that montite is more resorbable than brushite and does not convert to apatite, calcium phosphate cements are usually prepared in the form of brushites. This is because the precipitation of brushite is exothermic while montite gets prepared in an endothermic reaction.[25,31-33] With this in mind, understanding the structural properties of SA/HA composite and the role of each parameter in the final behavior of the composite will help try new methods in their fabrication. By the same token, Luo et al used a 3D plotting technique to fabricate a pre-designed porous structure of SA/HA nanocomposite. Their results demonstrated that an in-situ mineralization method was used for this structure leading to the enhancement of the mechanical properties and formation of a superficial nano-apatite which improved cell attachments.[34] They also showed that their prepared structure has a sustained protein delivery capability which is favorable for drug delivery purposes in tissue engineering. Moreover, there are tremendous numbers of documents which approve the effectiveness of using antibiotics together with bioceramics in treating bone infections.[35-37] Therefore, using a drug delivery system to carry the antibiotics to the bone's injured area is of importance due to the poor blood circulation around it. In the same way, a composite with an intrinsic antibacterial behavior is another solution for this issue. Surprisingly, the race between bio film formation and tissue cells adherence to the surface indicates the success level of an implantation as a substitute or graft in the injured site. Furthermore, the adhesion of tissue cells to the implant is a good sign of bioactivity of the implant's surface which will lead to a uniform healing of the injured region. To the knowledge of the authors there are no reports of antibacterial characterization of alginate and CaP in form of HA and brushite. Therefore, this study focused on the in-situ fabrication of the SA/brushite and SA/HA hydrogel composites as injectable antibacterial bone fillers. In particular, different synthesis methods as well as a final composition have been fully characterized to understand their bone filling properties. In this case, the compositions and structural properties were characterized by Fourier transform infrared (FTIR) spectroscopy, X-ray diffraction (XRD) analysis and scanning electron microscopy (SEM). Furthermore, the antibacterial activity of the hybrid composites was assessed against two common pathogenic bacteria including *Escherichia coli* and *Streptococcus agalactiae* through performing minimal bactericidal concentration (MBC) and the minimal inhibitory concentration (MIC) tests.

Materials and Methods

Hydroxyapatite Synthesis

In this study, Nano HA powder was synthesized via microwave assisted method and all the used reagents were of analytical grade and were applied without any further purification. Also, high-purity calcium nitrate tetrahydrate (Daejung chemicals and metals Co., Ltd., S. Korea) and ammonium phosphate dibasic (Daejung Chemicals and metals Co., Ltd., S. Korea) were used as the starting materials according to the stoichiometric ratio (1.67). First, the mixture was stirred for 30 minutes at room temperature and the pH

of the solution was adjusted to the degrees between 11 and 13 by adding ammonium hydroxide (1M, Merck). Further on, the mixture was placed in a customized domestic microwave oven equipped with a mechanical stirrer and a refluxing system and the radiation power and temperature was adjusted using a control panel made specifically for this device. The microwave oven was 800W (ALONSA, AL-520MW) with an input voltage of 220 V AC and 50 Hz single phase and 2450 MHz operating frequency. The temperature was set to 100°C and the microwave device was running for 20 minutes. After cooling down to room temperature, the precipitates were washed with copious amounts of ethanol and deionized water and filtered to remove the unreacted precursors. Eventually, the resultant precipitates were dried under vacuum at room temperature for 12 hours.

Preparations of Alginate-Brushite and Alginate-Hydroxyapatite Composite

To control the handling viscosity, carboxy-methyl-cellulose (CMC) of an analytical grade (Daejung Chemicals and metals Co., Ltd., S. Korea) was used as a thickener. Therefore, three groups of samples were prepared as follows: Group 1 (G1): in-situ alginate/Cap microspheres prepared in a calcium ion bath, group 2 (G2): in-situ alginate/CaP prepared in a CMC/calcium crosslinking media and group 3 (G3): the mixture of pre-synthesized HA and alginate in a calcium ion bath. Obviously, in all the three samples a 4% (W/V) alginate was used. In G1 0.0095 mole of ammonium phosphate dibasic was added to the alginate solution and the mixture was slowly added to the crosslinking bath (500 mL of 6% (W/V) calcium nitrate tetrahydrate) using a 22-gauge syringe. The pH was adjusted to 12 by adding ammonium solution dropwise. After 12 hours, the resultant microsphere was washed and filtered out.

Likewise, in G2 the same ratio of phosphate and SA was used but the crosslinking media was thickened with carboxy methyl cellulose. Thus, to prepare this crosslinking media, 25 ml of 2.5% (W/V) CMC was mixed with 37.5 mL of a 6% calcium nitrate tetrahydrate. Then, the alginate/phosphate mixture was poured into one side of a two-barrel syringe and the calcium/CMC into the other. As a result, the extruded mixture of the syringe was the paste of our interest (The pH was not determined).

Similarly, in G3 the pre-synthesized HA nano powder with the same ratio of phosphate to the alginate of G1 was added to the SA solution and thoroughly mixed to obtain a homogenous solution. Then, the solution was slowly added to calcium ion bath of 4% (w/v) via a 22-gauge syringe.

Afterwards, alginate-calcium phosphate (Alg/CaP) composite beads of G1 and G3 samples were washed thoroughly with distilled water to ensure no calcium residue had remained on the surface. All the samples were then freeze-dried overnight and stored in sealed plastic bags. For better clarification, Figure 1 illustrates the schematic of the three methods to prepare an Alg/CaP composite and the way it is supposed to be used in clinical applications. Also, Figure 2 illustrates the prepared Alg/CaP in forms of beads and mixed gel.

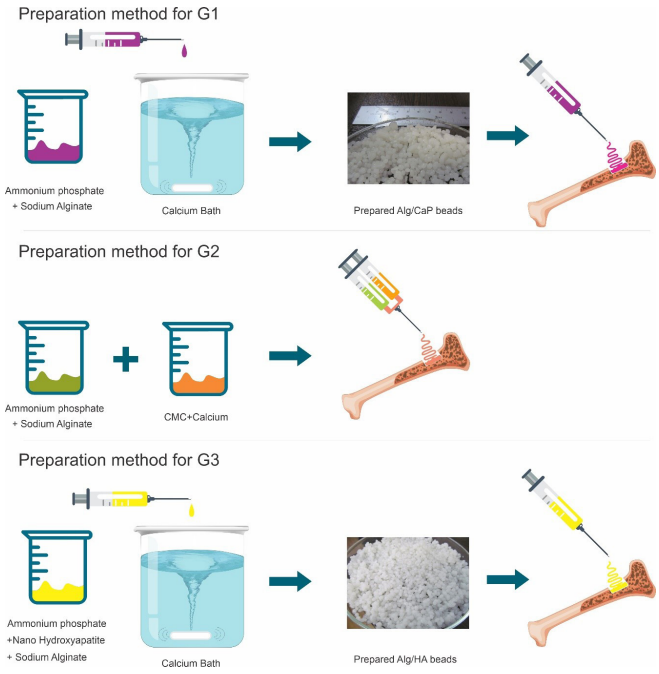

Figure 1. Schematic illustration of three methods to prepare Alg/CaP composite and the way it is supposed to be used in clinical applications. In G1 preparation, the mixture of alginate and ammonium phosphate was added dropwise to the crosslinking bath. To prepare G2 the mixture of alginate and ammonium phosphate and the mixture of CMC and calcium nitrate load to a two-barrel syringe and extruded. To prepare G3 the nano hydroxyapatite was mixed with mixture of alginate and ammonium phosphate and then was added dropwise to the crosslinking bath.

Figure 2. Digital photos of Alg/CaP in forms of bead and mixed gels. The picture on the top left shows prepared beads of G1, and the top right picture shows mixture of G3 sample. Bottom left picture shows nano hydroxyapatite powder synthesized by microwave method and the bottom right is the picture of beads of G3.

Characterization

The micro morphology of HA and HA/alginate was investigated by scanning them using an electron microscope (ESEM, XL30, Philips, Netherland). The samples included gold-sputtered with EMS 7620 SEM sputter coater (Quorom Technologies-Emitech). The SEM images were taken at the beam intensity of 20-30 kV. Fourier Transform IR (FT-IR) spectrum of samples was analyzed as KBr pellets using a

Thermo Nicolet NEXUS TM spectrophotometer. For XRD, microspheres were reduced to powder and analyzed with Cu Kα radiation using a Rigaku PMG-VH diffract meter.

Microorganisms and Culture Medium

Escherichia coli, and *S. agalactiae* were selected as representative gram negative and gram positive bacteria, respectively. All the strains were aerobic and were grown at 37°C. Mueller-Hinton broth and Mueller-Hinton agar (Merck, Germany) were used as a media to test the susceptibility of the bacteria.

Antimicrobial Activity Test

To carry out the microbial activity of SA/HA nanocomposite, the MIC and MBC tests were performed according to clinical and laboratory standards of the institute's guidelines.[38] To determine the MICs eight different concentrations, including 1000, 500, 250, 125, 63, 31, 16 and 8 µg/mL of broth were prepared by adding appropriate amounts of MH broth and one milliliter of each concentration was transferred to a test tube. After on, 1 mL of one of the three different suspensions with the inoculum concentration equivalent of 0.5 McFarland (almost 1 $\times 10^8$ CFU/mL) were added to the appropriate test tube. After 24 hours at 37°C, the turbidity of each sample was determined. To evaluate the MBC concentration, 1 mL of each incubated test tube was cultured on an MH agar plate at 37°C for 24 hours. Then, the bacterial growth was assessed and each test was performed in triplicate. The tubes without nanocomposites as a positive control and those without bacteria as a negative control were also examined.

Cytotoxicity Effects Analysis

The possible cytotoxic effect of the prepared nanocomposite was assessed using MTT (3-[4,5-dimethylthiazol-2-yl]-2,5-diphenyltetrazolium bromide) colorimetric assay. The MTT assay was performed by an indirect culture of bone marrow-derived mesenchymal stem cells on the leachates extracted from the sterile powders after 10 days according to the international standard ISO10993-12. The number of 1×10^4 cells/well were plated into 96-well plates and incubated at 37°C and 5% CO_2. After 24 and 48 hours of incubation, the medium of each well was removed and washed with phosphate buffered saline. The cells were incubated with 20 µL/well of MTT reagent for 4 hours at 37°C. Then the supernatants were replaced with 150 µL dimethyl sulfoxide (Sigma–Aldrich, Germany). The optical absorbance at 570 nm was measured using a microplate reader (ELISA reader, ELX808, BioTek). At least three samples were averaged for each group. Cells without extract were considered as control.

Results

Synthesis Characterization

Three types of SA/CaP composites were prepared by mixing similar solutions of SA 4% (w/v) with phosphate salt and a mixture of phosphate salt with carboxymethylcellulose and HA nano-powder, respectively. In all three samples, an equal amount of phosphate was used (by mole percent). In G1 the size of needle gauge and the stirring speed of the magnet in cross-linker bath had pivotal roles in shaping the SA/CaP white beads. Also, during the G1 preparation, adjusting the pH level was determinant due to the role of pH in the formation of calcium phosphate in the beads. On the other hand, by adding the alginate solution the pH of the crosslinking bath dropped to four. However, after using ammonium solution, the pH was adjusted to 12. Although in both media the beads were formed, the beads in media with a lower pH level had more transparency than the other ones. In order to characterize the SA/CaP composite beads, the one prepared in basic calcium ion bath was used. While preparing G2, the pH was maintained at seven which was favorable for brushite forming.

X-ray Diffraction

Various polymer composites have their own mechanisms for nucleation and growth of calcium phosphate. Thus, XRD and FTIR were applied for further characterization of the filler. Accordingly, the XRD pattern presented in Figure 3 demonstrates the three composites and the neat HA patterns. As it was expected, the XRD pattern of G3 and neat HA presented characteristic peaks of hydroxy apatite at 25.8, 31.9 and 39.6 attributed to the (002), (211), and (310), respectively. Peaks related to G1 and G2 represented brushite formation with characteristic peak at 2Theta of 29.5. Also, in G1 with

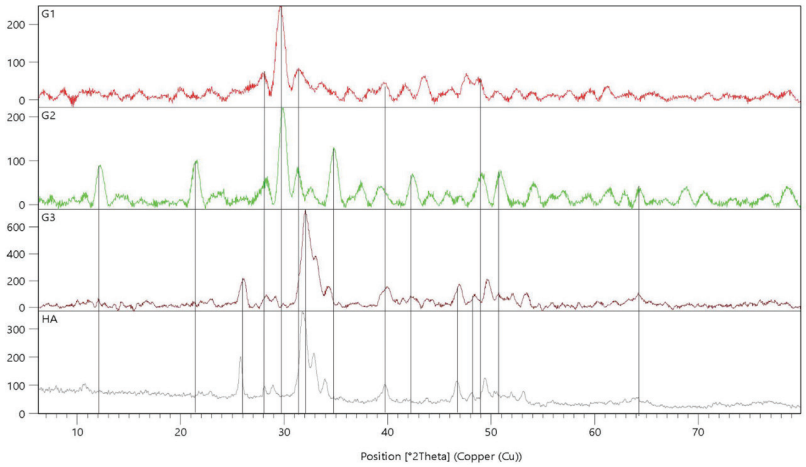

Figure 3. XRD Pattern of G1 (above), G2, G3 and Neat Hydroxyapatite.

an increase in the pH value some HA-related peaks were noticeable. In G2 two broad peaks at two theta of 12 and 21 were assumed to overlap with (020) and (021) of brushite and CMC-Alginate.

Fourier Transform Infrared

As demonstrated in Figure 4 and Table 1, the FTIR characterization showed a broad band in a region between 3000 and 3700 cm^{-1}, which was related to the oxygen and hydrogen in structure. Hence, the band around 3480 cm^{-1} region corresponded to the amount of the absorbed water in alginate and the HA and the others could be assigned to the OH- functional groups associated with groups such as phosphate. The strong absorbance around the 1630 and 1430 cm^{-1} is attributed to asymmetric and symmetric vibrations of carboxylates –COO groups in polymeric backbone, respectively. This indicates the presence of free carboxylate groups of biopolymer which act as nucleation sites for growing the hydroxy apatite. Furthermore, the absorption band for other C-O functionalities such as C-OH and C-O-C appear at 1384 and 1123 cm^{-1}, respectively.[39] Phosphate groups in CaPs have an absorption band in 1035, and also SA have a prominent absorption band in this region for their C-O-C stretching vibration. Thus, the overlap between these two causes a complex absorption band in the range of 1000 to 1200 cm^{-1}. The P-O band also has shown another absorption between 520 and 600. The peak at 1384 cm^{-1} represents the –C–O stretch of a primary alcoholic group (–CH_2–OH).

Antimicrobial Activity of Paste Analysis

Antimicrobial studies were carried out for two strains of bacteria – gram-negative *E. coli* and gram-positive *S. agalactiae*. The bactericidal effect of each of the three samples was assessed by exposing different concentrations of them in a broth medium to test the organisms. In this study, all three groups of SA/CaP composites in MH medium acted as bactericides against the *S. agalactiae*. *In situ* prepared SA/HA nanocomposites -G1 and G2- showed inhibitory effects in lower concentrations, 31 and 63 µg/mL, respectively. However, for the cross-linked mixture of pre-synthesized hydroxy apatite and SA, the antimicrobial activity was observed in a higher concentration of 125 µg/mL. The inhibitory effect of all the three samples for *E. coli* could not be determined in low concentrations and it was found out that G1 and G3 had bacteriostatic characteristics in concentrations up to 10000 µg/mL and 5000 µg/mL. The bactericidal concentrations for G1, G2 and G3 against the *S. agalactiae* were 125, 63 and 250 µg/mL, respectively. Similar to the MIC, the bactericidal effect of all three samples against the *E. coli* was found out to exist in concentrations higher than 10 000 µg/mL. It has been

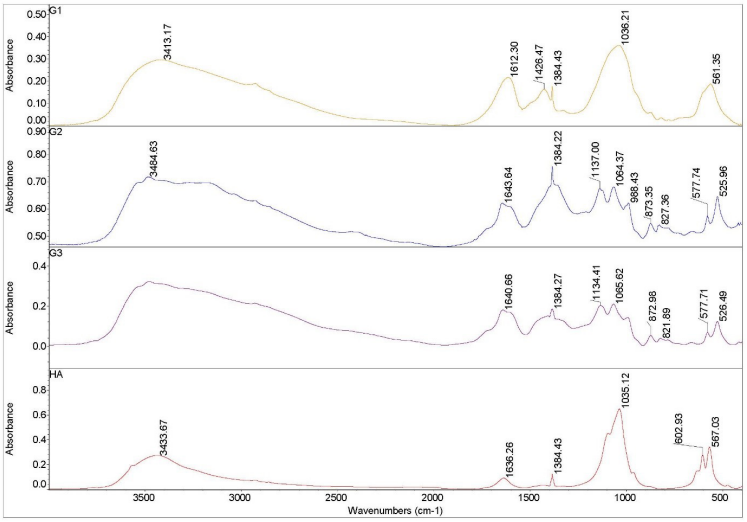

Figure 4. FTIR Spectrum of G1, G2, G3 and Neat Hydroxyapatite.

Table 1. Absorption Produced by Functional Groups Found in G1 to G3 and Neat HA

IR Absorption of Functional Groups		
Functional Group	**Absorption Location (cm^{-1})**	**Absorption Intensity**
O-H	3000-3700	Broad band
Water and OH- groups associated with groups such as phosphate	3480	Medium band
Asymmetric vibration of carboxylates –COO groups	1630	Medium
Symmetric vibration of carboxylates –COO groups	1430	Medium
C-O functionalities such as C-OH	1384	Strong peak
C-O functionalities such as C-O-C	1123	Strong Peak
Phosphate groups	1035	Strong Band
C-O-C stretching vibration	Around 1050	Prominent band

observed that SA/HA nanocomposite exhibits better activity against gram-negative *E. coli* as compared to gram-positive *S. agalactiae*. Table 2 shows the MIC and MBC values obtained for all three samples.

Cytotoxicity Effects of Paste Analysis

Figures 5 and 6 show the dead cells' percentage in MTT assay after 24 and 48 hours, respectively. With the increase of SA/CaP concentration, the cell death increases as well. However, G2 containing Alginate-CMC-brushite exhibits lower cell death even at higher concentrations. The most cell death percentage is related to the G3- the mixture of Ha and SA- which reached about full cell deaths after 48 hours. The lower concentration of all samples did not show any significant cell deaths.

Table 2. MIC and MBC Values Obtained for G1, G2 and G3

Paste con. (mg/mL)	MIC		MBC	
	E. coli	*S. agalactiae*	*E. coli*	*S. agalactiae*
G1	10	63	>10	125
G2	5	31	10	63
G3	10	125	10	250

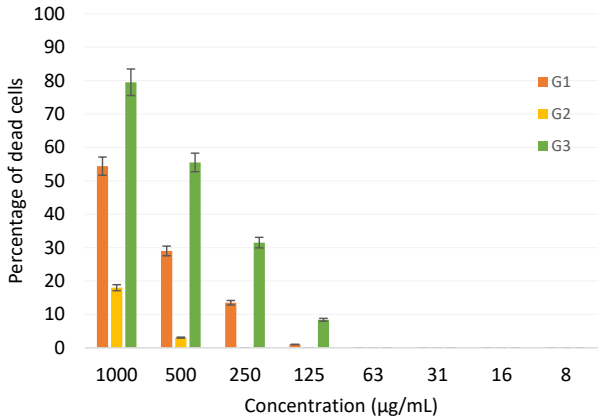

Figure 5. Percentage of Dead Cells After 24 Hours for Different Concentrations of G1, G2 and G3.

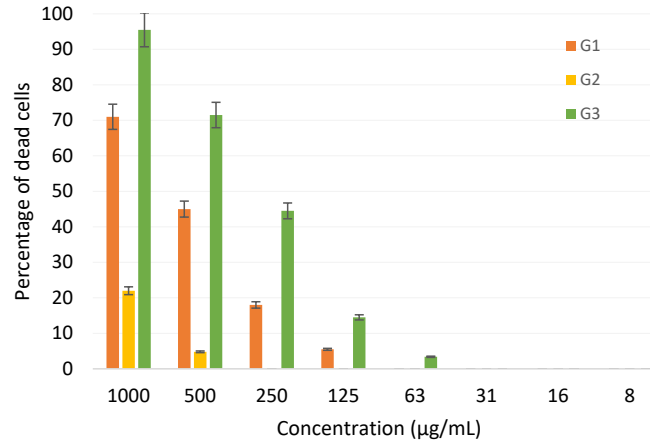

Figure 6. Percentage of Dead Cells After 48 Hours for Different Concentrations of G1, G2 and G3.

Scanning Electron Microscopy Analysis

SEM showed the microstructure of G1 in the first row, G2 in the second row and G3 in the third row (Figure 8). All the samples induced HA in their surfaces. It can be stated that G1 and G3 which had formed the shape of microspheres showed similar microstructures. Both mixtures had layered structures on their surfaces while G2 which was formed in the shape of a film had cubic crystals in ranges between 3 to 5 microns in size. The distribution of plates and cubes were uniform on all the surfaces.

Discussion

In this study, the antibacterial and cytotoxic behavior of three injectable calcium phosphate composite bone fillers was assessed. The main purpose of these fillers is their easy application by surgeons and the possession of an intrinsic antibacterial efficiency without the use of a drug delivery system. Therefore, as it was described before two different methods of fabricating a bio-composite made up of calcium phosphate in form of HA and brushite with biopolymer matrix have been developed. Furthermore, major differences between these two synthetic composites are attributed to the formation of calcium phosphate in their structures. For instance, in G1 and G2, brushite was produced by in-situ forming of sodium-alginate with calcium nitrate and calcium-nitrate-CMC solutions, respectively. However, G3 had HA synthesized with polycondensation method in a microwave oven and blended with SA solution, then cross-linked with calcium nitrate. Nevertheless, in both methods a syringe could be used and injected to the bone injury site. In addition, the required amount of HA powder in G3 was calculated based on the similar mole of phosphate salt used in G1 and G2. The fact that the materials used in this composite are biodegradable allows the filler to be substituted by a new bone without causing any foreign body reaction in the injected site. However, solubility and biodegradability of the brushite in comparison with HA, which has been reported by many researchers, requires further investigations to reveal the duration of its full degradation. On the other hand, results from XRD and FTIR spectrometry confirmed that brushite in G1 and G2 and HA in G3 were produced. The stronger peak intensity in the FTIR result of G1, G2 and G3 in comparison to neat HA is assumed to be related to the water and hydroxyl groups of alginate gel.[23] These abundant hydroxyl groups will lead to hydrogen bonds in SA/CaP composites which will contribute to the SA and calcium phosphate interfacial adhesion and will be observable in the OH- stretching vibration bands around 3440 cm-1.[23] Given these points, the bonding between CaP and SA is crucial for the mechanical performance of pastes especially for the ones including the brushite. Complex absorption band between 1000 and 1200 cm^{-1} is due to the overlap between the absorption peaks of phosphate groups in HA and C-O-C stretching vibration in alginate, which is reasonable to figure out the successful combination of SA/CaP in prepared composites.[6] Then, the final pastes are formed when the calcium salt is added for cross linking. Therefore, the composite produced in G1,

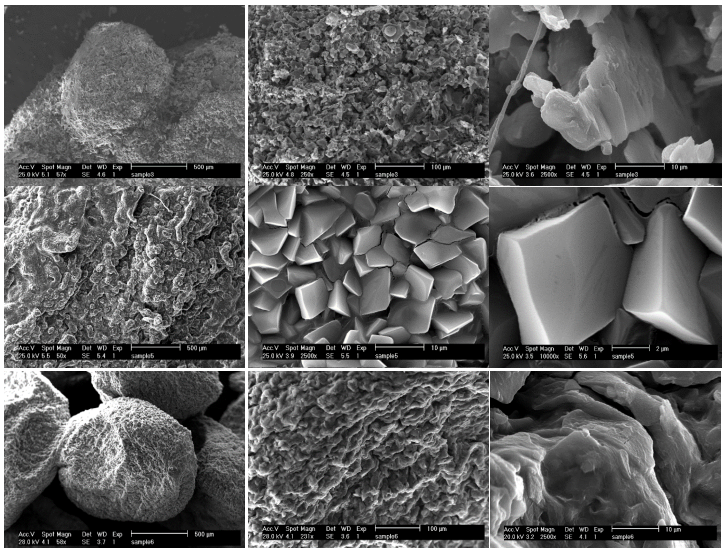

Figure 7. Scanning Electron Microscopy of G1 (first row), G2 (second row) and G3 (third row).

employed the dissolved calcium salt in the hardening bath to both forming the brushite and cross-link the alginate matrix. However, the results from FTIR and XRD indicate that the growth and nucleation of brushite in G1 were different from G2 and it seems that G1 is a mixture of brushite and apatite. Also, the crucial role of pH in G1 (above 9) should be considered as a main factor in these differences. However, further studies need to reveal the Ca concentration and Ca/P ratio and their optimized values. Then again, all three CaP composite samples (G1, G2 and G3) in this study exhibited antimicrobial activity. However, was resistive against these samples. Also, the lower antimicrobial activity against E. coli could be attributed to the fact that gram-negative in general is more resistant due to the external lipopolysaccharide wall surrounding the peptidoglycan cell wall.[40,41] As it has been mentioned in many research, the neat hydroxy apatite does not possess inhibitory effects.[42] Nonetheless, the other major components of the composite- SA with and without crosslinking agent of calcium ions- showed no antibacterial activity against both gram-negative and gram-positive bacteria strains.[41,43,44] Likewise, CMC had no antibacterial activity[45,46] and it was assumed that the incorporation of CMC into SA-brushite composite should reduce the antibacterial activity. As predicted, G2 had the least cytotoxicity level due to its ternary composition and showed higher antimicrobial activity which is favorable. Alginate-HA (G3) and G1 which consisted of calcium phosphate in both forms of apatite and brushite had higher cytotoxicity and antimicrobial effect in higher concentrations. Actually, in composition with brushite and CMC, alginate had a better antimicrobial than the other groups while it had no cytotoxicity in low concentrations or minimal cell death in higher concentrations compared to other groups.

Conclusions

In conclusion, calcium phosphate in form of brushite can be composited with biopolymers such as alginate and CMC to create a novel composition with antibacterial effects for bone filling applications. The special feature of this product is its intrinsic antibacterial efficiency in concentrations lower than 250 µg/mL while it did not inhibit cell growth. Additionally, the omission of metal nanoparticles such as silver-nanoparticles from main composition while maintaining antibacterial properties is another advantage of this product. To conclude, these properties not only reduce the risk of toxicity effect on mammalian cells but also, may improve the cell growth and make this composition a desirable filler for bone or tooth repair applications.

Authors' Contributions

All authors have participated in the experimental design, data collection, writing and revision of the manuscript.

Conflict of Interest Disclosures

The authors declare they have no conflicts of interest.

Acknowledgments

The authors would like to thank all the colleagues of Baqiyatallah University of Medical Sciences, Tehran, Iran for their support during this study.

References

1. Klinge B, Alberius P, Isaksson S, Jönsson J. Osseous response to implanted natural bone mineral and synthetic hydroxylapatite ceramic in the repair of experimental skull bone defects. J Oral Maxillofac Surg. 1992;50(3):241-249. doi:10.1016/0278-2391(92)90320-y.
2. Nakatsuka A, Yamakado K, Maeda M, et al. Radiofrequency ablation combined with bone cement injection for the treatment of bone malignancies. J Vasc Interv Radiol. 2004;15(7):707-712. doi:10.1097/01.rvi.0000133507.40193.e4.
3. Burg KJ, Porter S, Kellam JF. Biomaterial developments for bone tissue engineering. Biomaterials. 2000;21(23):2347-2359. doi:10.1016/s0142-9612(00)00102-2.
4. Vallet-Regí M, Salinas AJ. Ceramics as Bone Repair Materials. In: Bone Repair Biomaterials. Elsevier; 2019:141-178.
5. Burchardt H. The biology of bone graft repair. Clin Orthop Relat Res. 1983(174):28-42. doi:10.1097/00003086-198304000-00005.
6. Li H, Jiang F, Ye S, Wu Y, Zhu K, Wang D. Bioactive apatite incorporated alginate microspheres with sustained drug-delivery for bone regeneration application. Mater Sci Eng C Mater Biol

Appl. 2016;62:779-786. doi:10.1016/j.msec.2016.02.012.
7. Sato T, Kikuchi M, Aizawa M. Preparation of hydroxyapatite/collagen injectable bone paste with an anti-washout property utilizing sodium alginate. Part 1: influences of excess supplementation of calcium compounds. J Mater Sci Mater Med. 2017;28(3):49. doi:10.1007/s10856-017-5853-3.
8. Gauthier O, Boix D, Grimandi G, et al. A new injectable calcium phosphate biomaterial for immediate bone filling of extraction sockets: a preliminary study in dogs. J Periodontol. 1999;70(4):375-383. doi:10.1902/jop.1999.70.4.375.
9. Lindfors NC, Tallroth K, Aho AJ. Bioactive glass as bone-graft substitute for posterior spinal fusion in rabbit. J Biomed Mater Res. 2002;63(2):237-244. doi:10.1002/jbm.10177.
10. Ghassemi T, Shahroodi A, Ebrahimzadeh MH, Mousavian A, Movaffagh J, Moradi A. Current concepts in scaffolding for bone tissue engineering. Arch Bone Jt Surg. 2018;6(2):90-99. doi:10.22038/ABJS.2018.26340.1713.
11. Liao S, Wang W, Uo M, et al. A three-layered nano-carbonated hydroxyapatite/collagen/PLGA composite membrane for guided tissue regeneration. Biomaterials. 2005;26(36):7564-7571. doi:10.1016/j.biomaterials.2005.05.050.
12. Duan R, Barbieri D, Luo X, et al. Variation of the bone forming ability with the physicochemical properties of calcium phosphate bone substitutes. Biomater Sci. 2017;6(1):136-145. doi:10.1039/c7bm00717e.
13. Bohner M, Tadier S, van Garderen N, de Gasparo A, Döbelin N, Baroud G. Synthesis of spherical calcium phosphate particles for dental and orthopedic applications. Biomatter. 2013;3(2). doi:10.4161/biom.25103.
14. Dorozhkin SV, Epple M. Biological and medical significance of calcium phosphates. Angew Chem Int Ed Engl. 2002;41(17):3130-3146. doi:10.1002/1521-3773(20020902)41:17<3130::aid-anie3130>3.0.co;2-1.
15. Wang Q, Gu Z, Jamal S, Detamore MS, Berkland C. Hybrid hydroxyapatite nanoparticle colloidal gels are injectable fillers for bone tissue engineering. Tissue Eng Part A. 2013;19(23-24):2586-2593. doi:10.1089/ten.TEA.2013.0075.
16. González Ocampo JI, Machado de Paula MM, Bassous NJ, Lobo AO, Ossa Orozco CP, Webster TJ. Osteoblast responses to injectable bone substitutes of kappa-carrageenan and nano hydroxyapatite. Acta Biomater. 2019;83:425-434. doi:10.1016/j.actbio.2018.10.023.
17. Kumar AP, Mohaideen KK, Alariqi SAS, Singh RP. Preparation and characterization of bioceramic nanocomposites based on hydroxyapatite (HA) and carboxymethyl cellulose (CMC). Macromol Res. 2010;18(12):1160-1167. doi:10.1007/s13233-010-1208-3.
18. Donati I, Mørch YA, Strand BL, Skjåk-Braek G, Paoletti S. Effect of elongation of alternating sequences on swelling behavior and large deformation properties of natural alginate gels. J Phys Chem B. 2009;113(39):12916-12922. doi:10.1021/jp905488u.
19. Venkatasubbu GD, Ramasamy S, Ramakrishnan V, Kumar J. Hydroxyapatite-alginate nanocomposite as drug delivery matrix for sustained release of ciprofloxacin. J Biomed Nanotechnol. 2011;7(6):759-767. doi:10.1166/jbn.2011.1350.
20. Lu L, Qi Y, Zhou C, Jiao Y. Rapidly in situ forming biodegradable hydrogels by combining alginate and hydroxyapatite nanocrystal. Science in China Series E: Technological Sciences. 2010;53(1):272-277. doi:10.1007/s11431-009-0332-9.
21. Sotome S, Uemura T, Kikuchi M, et al. Synthesis and in vivo evaluation of a novel hydroxyapatite/collagen–alginate as a bone filler and a drug delivery carrier of bone morphogenetic protein. Mater Sci Eng C Mater Biol Appl. 2004;24(3):341-347. doi:10.1016/j.msec.2003.12.003.
22. Benedini L, Placente D, Pieroni O, Messina P. Assessment of synergistic interactions on self-assembled sodium alginate/nano-hydroxyapatite composites: to the conception of new bone tissue dressings. Colloid Polym Sci. 2017;295(11):2109-2121. doi:10.1007/s00396-017-4190-x.
23. Luo H, Zuo G, Xiong G, Li C, Wu C, Wan Y. Porous nanoplate-like hydroxyapatite–sodium alginate nanocomposite scaffolds for potential bone tissue engineering. Mater Technol. 2017;32(2):78-84. doi:10.1080/10667857.2015.1125045.
24. Tamimi F, Sheikh Z, Barralet J. Dicalcium phosphate cements: brushite and monetite. Acta Biomater. 2012;8(2):474-487. doi:10.1016/j.actbio.2011.08.005.
25. Dabiri SMH, Lagazzo A, Barberis F, Farokhi M, Finochio E, Pastorino L. Characterization of alginate-brushite in-situ hydrogel composites. Mater Sci Eng C Mater Biol Appl. 2016;67:502-510. doi:10.1016/j.msec.2016.04.104.
26. Dabiri SMH, Lagazzo A, Barberis F, Shayganpour A, Finocchio E, Pastorino L. New in-situ synthetized hydrogel composite based on alginate and brushite as a potential pH sensitive drug delivery system. Carbohydr Polym. 2017;177:324-333. doi:10.1016/j.carbpol.2017.08.046.
27. Luo J, Engqvist H, Persson C. A ready-to-use acidic, brushite-forming calcium phosphate cement. Acta Biomater. 2018;81:304-314. doi:10.1016/j.actbio.2018.10.001.
28. Grover LM, Knowles JC, Fleming GJ, Barralet JE. In vitro ageing of brushite calcium phosphate cement. Biomaterials. 2003;24(23):4133-4141. doi:10.1016/s0142-9612(03)00293-x.
29. Bjørnøy SH. Understanding Crystallization in Alginate-Calcium Phosphate Composites. NTNU; 2017.
30. Russell RG, Caswell AM, Hearn PR, Sharrard RM. Calcium in mineralized tissues and pathological calcification. Br Med Bull. 1986;42(4):435-446. doi:10.1093/oxfordjournals.bmb.a072163.
31. Bohner M, Gbureck U. Thermal reactions of brushite cements. J Biomed Mater Res B Appl Biomater. 2008;84(2):375-385. doi:10.1002/jbm.b.30881.
32. Bohner M, Merkle HP, Lemaître J. In vitro aging of a calcium phosphate cement. J Mater Sci Mater Med. 2000;11(3):155-162. doi:10.1023/a:1008927624493.
33. Gbureck U, Hölzel T, Klammert U, Würzler K, Müller FA, Barralet JE. Resorbable dicalcium phosphate bone substitutes prepared by 3D powder printing. Adv Funct Mater. 2007;17(18):3940-3945. doi:10.1002/adfm.200700019.
34. Luo Y, Lode A, Wu C, Chang J, Gelinsky M. Alginate/nanohydroxyapatite scaffolds with designed core/shell structures fabricated by 3D plotting and in situ mineralization for bone tissue engineering. ACS Appl Mater Interfaces. 2015;7(12):6541-6549. doi:10.1021/am508469h.
35. Yu J, Chu X, Cai Y, Tong P, Yao J. Preparation and characterization of antimicrobial nano-hydroxyapatite composites. Mater Sci Eng C Mater Biol Appl. 2014;37:54-59. doi:10.1016/j.msec.2013.12.038.
36. Bansal R, Jain A. Overview on the current antibiotic containing agents used in endodontics. N Am J Med Sci. 2014;6(8):351-358. doi:10.4103/1947-2714.139277.
37. Zheng F, Wang S, Wen S, Shen M, Zhu M, Shi X. Characterization and antibacterial activity of amoxicillin-loaded electrospun nano-hydroxyapatite/poly(lactic-co-glycolic acid) composite nanofibers. Biomaterials. 2013;34(4):1402-1412. doi:10.1016/j.biomaterials.2012.10.071.
38. Wikler MA. Methods for Dilution Antimicrobial Susceptibility Test for Bacteria That Grow Aerobically. Clinical and Laboratory Standards Institute; 2009;.
39. Wang J, Liu C, Shuai Y, Cui X, Nie L. Controlled release of anticancer drug using graphene oxide as a drug-binding effector in konjac glucomannan/sodium alginate hydrogels. Colloids Surf B Biointerfaces. 2014;113:223-229. doi:10.1016/j.colsurfb.2013.09.009.
40. Burt S. Essential oils: their antibacterial properties and potential applications in foods--a review. Int J Food Microbiol. 2004;94(3):223-253. doi:10.1016/j.ijfoodmicro.2004.03.022.
41. Alboofetileh M, Rezaei M, Hosseini H, Abdollahi M. Antimicrobial activity of alginate/clay nanocomposite films enriched with

essential oils against three common foodborne pathogens. Food Control. 2014;36(1):1-7. doi:10.1016/j.foodcont.2013.07.037.
42. Jadalannagari S, Deshmukh K, Ramanan SR, Kowshik M. Antimicrobial activity of hemocompatible silver doped hydroxyapatite nanoparticles synthesized by modified sol–gel technique. Appl Nanosci. 2014;4(2):133-141. doi:10.1007/s13204-013-0197-x.
43. Cha DS, Choi JH, Chinnan MS, Park HJ. Antimicrobial films based on Na-alginate and κ-carrageenan. LWT Food Sci Technol. 2002;35(8):715-719. doi:10.1006/fstl.2002.0928.
44. Pranoto Y, Salokhe VM, Rakshit SK. Physical and antibacterial properties of alginate-based edible film incorporated with garlic oil. Food Research International. 2005;38(3):267-272. doi:10.1016/j.foodres.2004.04.009.
45. Yadollahi M, Gholamali I, Namazi H, Aghazadeh M. Synthesis and characterization of antibacterial carboxymethyl cellulose/ZnO nanocomposite hydrogels. Int J Biol Macromol. 2015;74:136-141. doi:10.1016/j.ijbiomac.2014.11.032.
46. Hu D, Wang H, Wang L. Physical properties and antibacterial activity of quaternized chitosan/carboxymethyl cellulose blend films. LWT Food Sci Technol. 2016;65:398-405. doi:10.1016/j.lwt.2015.08.033.